CIÊNCIA& TECNOLOGIA
ISSN: 2525-6599
unifev pesquisa
Coordenação de Pesquisa

INVESTIGATION OF SOIL IONIZATION EFFECTS ON TRANSIENT OVERVOLTAGES IN TRANSMISSION LINES SUBJECTED TO LIGHTNING STRIKES

Tainá Fernanda Garbelim Pascoalato[1]
Anderson Ricardo Justo de Araújo[2]

Resumo:
Este artigo investiga o efeito da ionização do solo no sistema de aterramento composto por eletrodos de contrapeso, combinando uma modelagem realista dos parâmetros de retorno pelo solo e seu impacto nas sobretensões geradas nas cadeias de isoladores de uma linha de transmissão aérea de 138 kV. Essa linha é submetida a uma descarga atmosférica modelada como uma fonte de corrente do tipo primeira descarga de retorno. O sistema de contrapeso do pé da torre tem um comprimento de 100 m e está enterrado em solos homogêneos, para os quais foram assumidas resistividades de 1.000 e 4.000 Ω.m e uma permissividade relativa ε_r de 10. A impedância impulsiva, com e sem o efeito de ionização, foi considerada para três valores do campo elétrico crítico: 200, 400 e 800 kV/m. As sobretensões no domínio do tempo foram calculadas utilizando o software ATP-EMTP®. Os resultados da simulação mostram que as formas de onda da sobretensão dependem da resistividade do solo e do campo elétrico crítico adotado para representar o sistema de aterramento do pé da torre. À medida que o campo elétrico crítico aumenta, a impedância do pé da torre também aumenta e as sobretensões se aproximam daquelas obtidas sem o efeito de ionização.

Palavras-chave: desempenho sob descargas atmosféricas; ionização do solo; modelagem de aterramento; transitórios eletromagnéticos.

Abstract
This paper investigates the soil ionization effect in the grounding system composed of counterpoise electrodes, combining a realistic modelling of ground-return parameters and its impact on the overvoltages generated in the insulator strings of a 138-kV overhead transmission line (OHTL) subjected to a lightning current representative of a first return stroke. The tower footing counterpoise system has a length of 100 m and is buried in homogeneous soils with resistivities of 1,000 and 4,000 Ω.m and relative permittivity ε_r of 10 were assumed. The impulse impedance, with and without the ionization effect, was considered for three values of the critical electric field E_c: 200, 400, and 800 kV/m. The time-domain overvoltages were calculated using the ATP-EMTP® software. Simulation results show that the overvoltage waveforms depend on the soil resistivity and the critical electric field adopted for representing the tower-footing grounding system. As the critical electric field increases, the tower-footing impedance also increases, and the overvoltages approach those obtained without the ionization effect.

[1] Centro Universitário de Votuporanga (Unifev). Votuporanga, São Paulo, Brasil. Doutora em Engenharia Elétrica. Email: tfgpascoalato@gmail.com.
[2] Universidade Estadual de Campinas (Unicamp). Campinas, São Paulo, Brasil. Doutor em Engenharia Elétrica. Email: ajaraujo@unicamp.br.

Keywords: electromagnetic transients; lightning performance; grounding modelling; soil ionization.

INTRODUCTION

The inclusion of the soil ionization effect is essential for accurately determining the impedance of a grounding system and the earth potential generated in response to impulsive currents injected in it. Moreover, grounding impedance is one of the key factors influencing the occurrence of backflashovers in overhead transmission lines (OHTL) (Souza, Silveira and Visacro, 2014; Sengar and Chandrasekaran, 2024; Silva, Visacro and Silveira, 2022).

Soil ionization occurs when the current density flowing from the grounding electrode causes the electric field intensity to exceed its critical value (He *et al.* 2005). As a result, the resistivity of the soil surrounding the conductor decreases, leading to a reduction in grounding impedance, which affects the overvoltages developed in the system (Souza, Silveira and Visacro 2014). Furthermore, in high-resistivity soils, lightning strikes can generate stronger electric fields, increasing the likelihood of ionization and modifying the impulse impedance. Several models incorporating soil ionization have been proposed in the literature (Kisielewicz and Cuenca, 2022; Mokhtari and Gharehpetian, 2017; Mokhtari, Abdul-Malek and Gharehpetian, 2016; Meyberg, de Barros and Mahseredjian, 2024). One of the main approaches involves modifying conductor dimensions based on an equivalent radius that depends on the critical electric field (Sengar and Chandrasekaran, 2024; He *et al.* 2005; Kisielewicz and Cuenca, 2022). Additionally, regarding OHTL, the Universal Line Model has been established as the most accurate representation and has recently been integrated into the ATP-EMTP software (Morched, Gustavsen and Tartibi, 1999). Traditionally, in this software, Carson's approach (Carson, 1926) is employed to compute the ground-return impedance in line modeling. However, more precise methods, such as Nakagawa's approach (Nakagawa, 1981), should be considered, as they account for displacement currents and frequency-dependent electrical parameters (resistivity and permittivity). In this context, combining realistic soil characteristics, such as soil ionization, with more advanced ground-return models leads to more accurate transient response simulations of OHTLs subjected to lightning strikes.

This study examines the influence of soil ionization in a grounding configuration consisting of counterpoise electrodes, integrated with a precise representation of ground-return parameters using Nakagawa's approach, on the overvoltages induced in the insulator assemblies of a 138-kV OHTL subjected to a lightning strike. The counterpoise grounding is buried in

uniform soil conditions with resistivities of 1,000 and 4,000 Ω.m, assuming a relative permittivity (ε_r) of 10. The impulse impedance, both with and without ionization influence, was evaluated for three threshold values of the critical electric field E_c: 200, 400, and 800 kV/m. The time-domain voltage surges were computed using ATP-EMTP software. The simulation findings indicate that the waveform of the overvoltages is strongly dependent on the soil resistivity and the chosen critical electric field for modeling the ionization effect on the tower-footing grounding system. As the critical electric field increases, the impulse impedance at the tower base rises, causing the overvoltages to converge toward those calculated without considering the ionization phenomenon.

1 SOIL MODELING

1.1 Ionization effect

During the process of current dissipation through the grounding system, an elevate potential (voltage) rise is generated on the metallic conductors. This electric voltage gives rise to a non-uniform electric field on the conductor's surface (Meyberg, de Barros and Mahseredjian, 2024). If the generated electric field E (V/m) exceeds the critical threshold field E_c, a dielectric breakdown of the soil is induced around a certain section of the conductor's surface from a radial distance. This surface is interpreted as a new current conduction area for that particular section of the electrode (He *et al.* 2005). This section, referred to as the ionized region, as shown in Fig. 1, can be interpreted as a nonlinear conductive medium surrounding the original section of the grounding conductor. This process results in a reduction of electrical resistivity in the ionized region, allowing a greater electric current to dissipate in this segment. This phenomenon can be interpreted as if the electrode assumes a larger diameter than its original value.

Figure 1 - Ionization region around the earthing electrode during lightning impulse

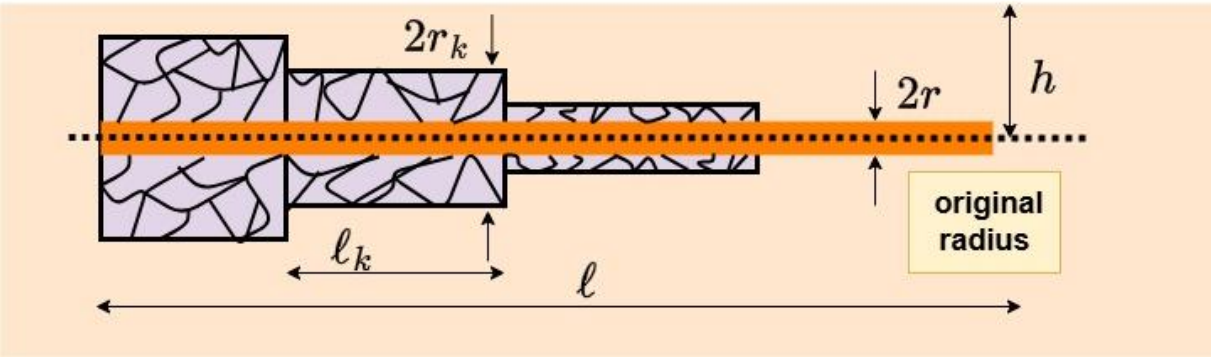

Source: Author's own work (2025).

Scientific studies in the literature have shown that resistivity is the only parameter altered in the ionization process whereas electric permittivity and magnetic permeability are not significantly altered (Gazzana *et al*. 2014). As a practical effect, soil ionization leads to a reduction in the potential rise in the soil for a given impulsive current injected into this conductor. If the electric field E (V/m) on the surface of the conductor exceeds a certain threshold ($E > E_c$), where E_c is the critical electric field (V/m), an increase in the effective radius of the conductor around the ionized region is established. Based on the transmission line representation, this increase in the diameter implies the need to modify the electrical parameters per unit length, conductance (G), and capacitance (C) of the electrode, viewed as a transmission line. Thus, the electrode is composed of a set of small ionized sections (segments), represented by concentrated cylinders, as shown in Fig. 1. The soil ionization is considered uniform around the ionized region, represented by the area corresponding to the increase in the radius of the electrode, compared to the electrode with an original radius r. The current density, in the critic electric field E_c (V/m), for the ionized region, is given by (Sengar and Chandrasekaran, 2024):

$$J_{io} = \frac{E_c}{\rho_{soil}} = \frac{I_{io}}{2\pi l_k r_k}, \quad (1)$$

where J_{io} is the current density of the conductor (A/m^2), ρ_{soil} (Ω.m) is the soil resistivity, I_{io} (A) is the current in the surface of the conductor, l_k (m) is the length of ionized section of the electrode and r_k (m) is the radius of this section, as depicted in Fig. 1. The increased radius of each ionized region is calculated as follows:

$$r_k = \frac{1}{2\pi}\frac{I_{io}}{E_c}\frac{\rho_{soil}}{l_k}. \quad (2)$$

This equivalent section surrounds the segments of the electrode which represents of the main models employed in the literature for modelling soil ionization effect.

1.2 Grounding impedance representation

The harmonic impedance of a grounding system must be calculated using the incremented electrode radius for the ionized region for a wide frequency range, taking into account the soil parameters. In this context, using several electromagnetic approaches to solve Maxwell's equations solved by numerical methods using full-wave electromagnetic software, such as FEKO (Altair-Hyperworks, 2023) using Method of Moments (MoM) (de Azevedo, de Araújo and Pissolato Filho, 2023), COMSOL using the Finite Element Method (FEM) (Bezerra, Moreira, Ferreira and Alípio, 2024), XGSLAB (XGSLab) hybrid using the Partial Equivalent Element Circuit (PEEC). Furthermore, programming codes were developed based on: MoM, such as the Hybrid Electromagnetic Model (HEM) (Silva, Visacro and Silveira, 2022; Silva, Visacro and Silveira 2023; Alemi, Sadeghi and Askarian-Abyaneh, 2022; Alemi, Sadeghi and Askarian-Abyaneh, 2023) or time-domain methods, such as Finite-Difference Time-Domain (FDTD) combined with models based on equivalent circuit using transmission line model or directly code modeling (Kisielewicz and Cuenca, 2022, Meyberg, de Barros and Mahseredjian, 2024; Gazzana *et al*. 2014; Gazzana *et al.* 2017; Nekhoul, Harrat, Boutadjine and Melit, 2022) for representing simple conductors have been largely used to assess the grounding impedance (transient impedance or the impulse impedance) in the literature. The potential developed due to an injected impulse current is denoted the Ground Potential Rise (GPR) relative to a remote point at infinity. The grounding impedance can be represented by a pure resistance, denoted as impulse impedance (Z_{p}), calculated by (He *et al.* 2005; Grcev, 2008):

$$Z_{\mathrm{p}} = \frac{V_{\mathrm{p}}}{I_{\mathrm{p}}}, \tag{3}$$

where V_{p} and I_{p} are the peak values of the transient GPR relative to the remote point and the injected current $i(t)$ in the grounding system, respectively. The impulse impedance is employed to represent the tower-footing grounding impedance in this work as further detailed.

2 OVERHEAD TRANSMISSION LINES

An OHTL of n phases can be modelled by its longitudinal impedance $\boldsymbol{Z}(\omega)$ and transversal admittance $\boldsymbol{Y}(\omega)$ $(n \times n)$ matrices given as follows:

$$\boldsymbol{Z}(\omega) = \boldsymbol{Z}_{\text{int}}(\omega) + \frac{j\omega\mu_0}{2\pi}\left[\ln\left(\frac{{D_{\text{ij}}}'}{d_{\text{ij}}} + \boldsymbol{S}_1\right)\right], \tag{4}$$

$$\boldsymbol{Y}(\omega) = j\omega\left\{\frac{1}{2\pi\varepsilon_0}\left[\ln\left(\frac{{D_{\text{ij}}}'}{d_{\text{ij}}} + \boldsymbol{S}_2\right)\right]\right\}^{-1}, \tag{5}$$

where $\omega = 2\pi f$ is the angular frequency (rad/s), f is the frequency (Hz), $\boldsymbol{Z}_{\text{int}}(\omega)$ is the internal impedance (Ω/m), taking the Skin Effect on the phase conductors. The ${D_{\text{ij}}}'$ is the distance between the conductor i and the image of adjacent conductor j (m), d_{ij} is the distance between conductors i and j (m). The electrical parameters are: μ_0 is the vacuum magnetic permeability $\mu_0 = 4\pi \times 10^{-7}$ (H/m), ε_0 is the vacuum permittivity $\varepsilon_0 = 8.85 \times 10^{-12}$ (F/m). The matrices $\boldsymbol{S}_1$ and $\boldsymbol{S}_2$ are derived from the Wise's and Nakagawa's formulation, being calculated as (Nakagawa, 1981):

$$\boldsymbol{S}_1 = 2\int_0^{\infty} \frac{e^{-(h_{\text{i}}+h_{\text{j}})\lambda}}{\sqrt{\lambda^2 + \gamma_{\text{g}}^2} + \lambda}\cos(r_{\text{ij}}\lambda)d\lambda, \tag{6}$$

$$\boldsymbol{S}_2 = 2\int_0^{\infty} \frac{e^{-(h_{\text{i}}+h_{\text{j}})\lambda}}{\sqrt{\lambda^2 + \gamma_{\text{g}}^2 + \eta_{\text{g}}^2\lambda}}\cos(r_{\text{ij}}\lambda)d\lambda, \tag{7}$$

where γ_{g}^2 and η_{g}^2 are given by (De Conti and Emídio, 2016):

$$\gamma_{\text{g}}^2 = j\omega\mu_0\left[\sigma_{\text{g}} + j\omega(\varepsilon_{\text{r}} - k)\varepsilon_0\right], \tag{8}$$

$$\eta_{\text{g}}^2 = \frac{\gamma_{\text{m}}^2}{\gamma_0^2} = -\frac{j\omega\mu_0(\sigma_{\text{g}} + j\omega\varepsilon_{\text{r}}\varepsilon_0)}{\omega^2\mu_0\varepsilon_0}, \tag{9}$$

where h_{i} and h_{j} are the heights of the conductors i and j in relation to the ground level (m), r_{ij} is the horizontal distance between the conductors i and j (m), λ is na integration variable, σ_{g} is the soil conductivity (S/m) and ε_{r} is the relative permittivity of soil. Note that k is a correction factor. If k = 1 in (8), the (6) and (7) are represented by Nakagawa's formulation (Nakagawa, 1981). Otherwise, if $k = \varepsilon_{\text{r}}$, (6) is reduced to classical Carson's formulation (Carson, 1926), where the displacement currents are neglected.

In the phase-domain, the OHTL can be represented by the Universal Line Model (ULM) (Morched, Gustavsen and Tartibi, 1999), where the voltages and currents along the line length are ruled by the frequency-dependent propagation function **H** and characteristic admittance matrix $\mathbf{Y}_{\text{c}}$, which are given as (Morched, Gustavsen and Tartibi, 1999):

$$\mathbf{H}(\omega) = e^{-\sqrt{\mathbf{YZ}}\ell}, \tag{10}$$

$$\mathbf{Y}_{\text{c}}(\omega) = \mathbf{Y}^{-1}\sqrt{\mathbf{YZ}}, \tag{11}$$

where ℓ is the line length. To calculate the voltages and currents along the OHTL, the frequency-dependent functions $\mathbf{H}$ and $\mathbf{Y}_c$ can be approximated by rational functions employing the Vector Fitting technique (Gustavsen and Semlyen, 1999). Following the procedure detailed by Zanon Leal and De Conti (2021), the $\mathbf{H}$ and $\mathbf{Y}_c$ can be written in their fitted functions given as:

$$\mathbf{H}(s) \approx \mathbf{H}_{\text{fit}} = \sum_{j=1}^{N_{\text{mod}}} \left(\sum_{n=1}^{N} \frac{\mathbf{c}_{nj}}{s - p_n} \right) e^{-s\tau_j}, \tag{12}$$

$$\mathbf{Y}_c(s) \approx \mathbf{Y}_c = k_0 + \sum_{n=1}^{N_p} \frac{\mathbf{k}_n}{s - p_n}, \tag{13}$$

where s is the complex frequency ($s = j\omega$) (rad/s), τ_j is the delay time (s), N is the number of poles required, N_{mod} is the total number of modes, $\mathbf{c}_{nj}$ are the matrices of residuals and p_n is the poles. Regarding (13), k_0 is a real matrix, $\mathbf{k}_n$ is the residues associated with each element of $\mathbf{Y}_c$ and N_p is the number of poles required for this fitting. For the implementation of ULM in ATP-EMTP®, the MATLAB® software is used, where the longitudinal impedance and transversal admittance matrices are calculated based on the geometric and soil data for a certain OHTL by the users. From this, the characteristic admittance, the propagation function, and the minimum delay times are obtained using *Vector Fitting*, from which the poles, residues, and other constants are determined. These parameters are organized in the form of a data file (.dat) and are then read by the PCH component, which represents the OHTL directly in ATP-EMTP®. The other components of the power system are connected, and simulations are performed directly in the time domain.

3 NUMERICAL RESULTS

The overvoltages generated in a 138-kV transmission line with a tower subjected to a lightning current representative of first return stroke (FRS) are evaluated under two different approaches:

- **Approach without ionization:** For the line model, the ULM is implemented using MATLAB® and ATP-EMTP® software, following the procedure described in Leal, De Conti and Zanon (2024). In this approach, $k = \varepsilon_r$, that is, the equations (6), (7) and (8) are calculated using Carson's formulation and the displacement currents is neglected. Furthermore, the soil resistivity (ρ_{soil}) is considered constant, with values of 1,000 and

4,000 Ω.m, and soil ionization is disregarded.

- **Approach with ionization:** For the line model, the ULM is implemented using MATLAB® and ATP-EMTP® software, following the procedure described in Leal, De Conti and Zanon (2024). In this approach, k = 1, that is, the equations (6), (7) and (8) are calculated using Nakagawa's formulation. Additionally, the soil resistivity (ρ_{soil}) is considered frequency-constant, with values of 1,000 and 4,000 Ω.m, the relative permittivity (ε_r) is set to 10, and soil ionization is considered (E_c = 200, 400, and 800 kV/m).

The values of Z_p were calculated by Sousa, Silveira and Visacro (2014) and they are organized in Tables 1 and 2.

Table 1 – Impulse impedance Z_p (Ω) for soil of 1,000 Ω.m

ρ = 1,000 (Ω.m)	E_c (kV/m)			
	No ionization	200	400	800
Z_p (Ω)	12.5	10.0	10.8	11.4

Source: Adapted of Souza, Silveira and Visacro (2014).

Table 2 – Impulse impedance Z_p (Ω) for soil of 4,000 Ω.m

ρ = 4,000 (Ω.m)	E_c (kV/m)			
	No ionization	200	400	800
Z_p (Ω)	30.8	25.4	28.3	29.7

Source: Adapted of Souza, Silveira and Visacro (2014).

To quantify the impact of ionization on the overvoltages generated in a transmission tower subjected to a lightning strike, the time-domain simulations for both soil approaches (with and without ionization effect for the tower-footing grounding system composed of counterpoise electrodes) are presented as follows. The tower silhouette and the circuit implemented in ATP-EMTP are presented in Figs. 2 and 3. Each component was modelled as follows: First, the representative of a first return stroke (FRS) is modelled as a sum of m Heidler functions, given by (De Conti and Visacro, 2007):

$$i(t) = \sum_{k=1}^{m} \frac{I_{0k}}{\eta_k} \frac{(t/\tau_{1k})^{n_k}}{1 + (t/\tau_{1k})^{n_k}} e^{-t/\tau_{2k}}, \quad (14)$$

$$\eta_k = e^{\left[-\left(\frac{\tau_{1k}}{\tau_{2k}}\right)\left(n_k\frac{\tau_{2k}}{\tau_{1k}}\right)\right]^{1/n_k}}, \quad (15)$$

where I_{0k} is the peak current value (A), τ_{1k} is the rise time constant (s), τ_{2k} is the decay time constant (s), η_k is a correction factor for I_{0k}, and n_k is a parameter related to the waveform slope (Heidler, 1985). The parameters of the lightning strike with its seven terms (m = 7) are detailed in De Conti and Visacro (2007) and showed in Table 3, and the time-domain current waveform is illustrated in Fig. 4.

Figure 2 – Transmission tower dimension and multi-conductor tower model

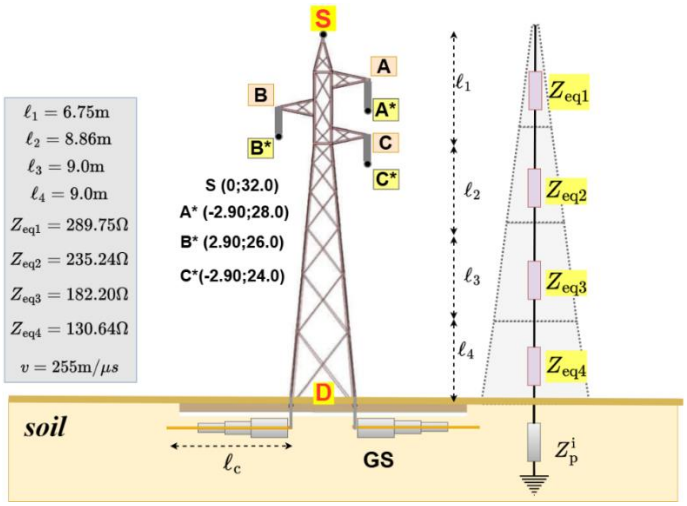

Source: Adapted from Schroeder, Moura Assis and Paulino (2023).

Figure 3 –Power system circuit model in ATP-EMTP

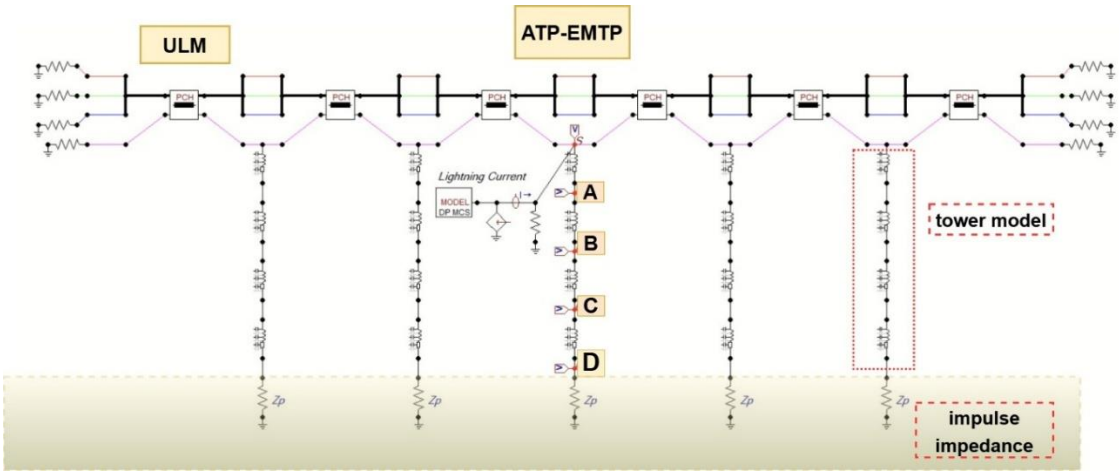

Source: Author's own work.

Table 3 – Parameters of the first return stroke (FRS)

Current type	k	I_0(kA)	n	$\tau_1(\mu s)$	$\tau_2(\mu s)$
First Return Stroke (FRS) ($T_{10} = 5.20\ \mu s, T_{30} = 3.0\ \mu s$)	1	6	2	3	76
	2	5	3	3.5	10
	3	5	5	4.8	30
	4	8	9	6	26
	5	16.5	30	7	23.2
	6	17	2	70	200
	7	12	14	12	26

Source: Adapted of De Conti and Visacro (2007).

Figure 4 – Lightning current representative of the first return stroke (FRS) used for the simulations

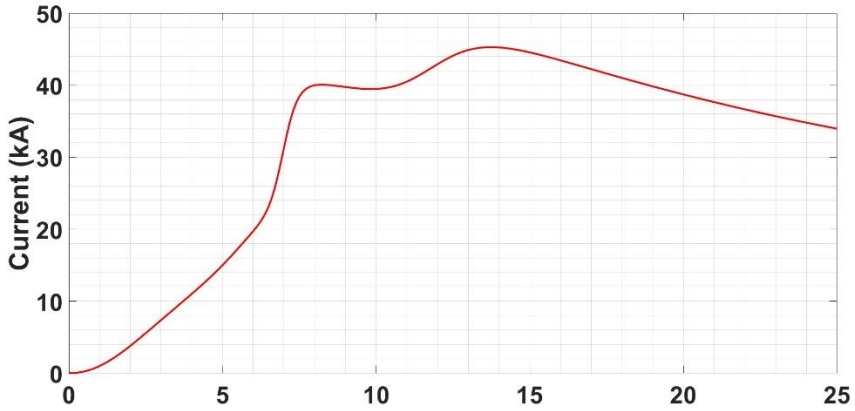

Source: Author's own work (2025).

The lightning strike is modelled as a current source associated with a channel impedance, modelled as purely resistive of 400 Ω, injected at the top of the transmission tower. The Fig. 5 illustrates the tower-footing grounding configuration adopted for the numerical simulations. It is composed of four grounding horizontal electrodes with radius r of 0.9 cm radius, buried at depth h of 0.50 m, distance between tower feet b of 7 m, and length ℓ_c of 100 m. The soil parameters are assumed with resistivities of 1,000 and 4000 Ω.m and relative permittivity ε_r of 10. The tower configuration, with the phase conductors located at A*, B*, and C*, and the grounding wire **S**, is illustrated in Fig. 2. The multi-conductor model represents each section of the tower structure as a lossless single line, with an equivalent surge impedance Z_{eq} associated with a propagation velocity (v = 0.85 c, c = 300 m/μs), as shown in Fig. 2. The

values of Z_{eq} are detailed in Schroeder, Moura, Assis and Paulino (2023) [See Fig. 2 of this article]. The resistance per unit length of the phase conductors is 0.21 Ω/km, and for the grounding wire, it is 2.175 Ω/km (Schroeder, Moura, Assis and Paulino, 2023).

Figure 5 – Tower footing grounding system composed of counterpoise electrodes: (a) side view; (b) top view

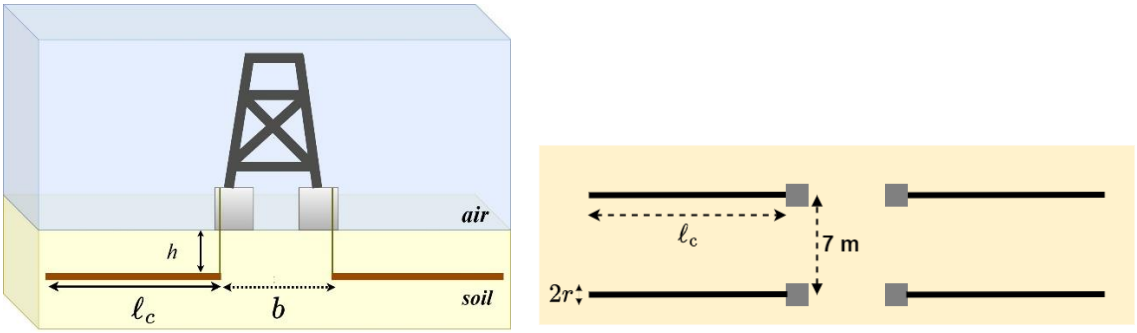

(a) **(b)**

Source: Author's own work (2025).

The grounding system is buried in soil modelled by its constant electrical parameters (resistivity and permittivity). The grounding impedance at the tower base is represented by the impulse impedance Z_p. The grounding system at the tower base used in this study is shown in Fig. 5, based on the article Souza, Silveira and Visacro (2014). Based on this topology, the grounding impedance was calculated using the HEM with and without the effect of soil ionization, assuming resistivities of 1,000 and 4,000 Ω.m. The impulse impedance values Z_p obtained for soils of 1,000 and 4,000 Ω.m, with and without the ionization effect, considering three values of critical electric field E_c of 200, 400, and 800 kV/m, are presented in Tables 1 and 2, respectively. According to these tables, the impulse impedance Z_p increases as the critical electric field E_c rises, approaching the value obtained when the ionization effect in the soil is disregarded. The greatest difference occurs at E_c = 200 kV/m, where Z_p is 20% and 17.5% higher compared to the values without soil ionization for soil resistivities of 1,000 Ω.m and 4,000 Ω.m, respectively (Souza, Silveira and Visacro, 2014).

The power system is implemented in ATP-EMTP simulation tool, as illustrated in Fig. 3. The analysed system consists of five transmission towers with four spans of 400 m each. Two 20 km lines are connected at each end to prevent reflections of voltage and current waves. The transmission line model is used to implement the line span, considering both approaches: with and without soil ionization in the grounding system. Five towers are defined using the

multi-conductor model, with their grounding impedances at the tower base modelled by Z_p, both with and without the ionization effect. The overvoltages generated at points A, B, and C by a lightning strike of type FRS in this power system are presented in Fig. 6.

Figure 6 – Transient voltages across the insulator string of 138-kV transmission line [left-side column for soil with ρ_{soil} = 1 kΩ.m and right-side column for soil with ρ_{soil} = 4 kΩ.m] at points: (a)-(b) **A**; (c)-(d) **B**; (e)-(f) **C**

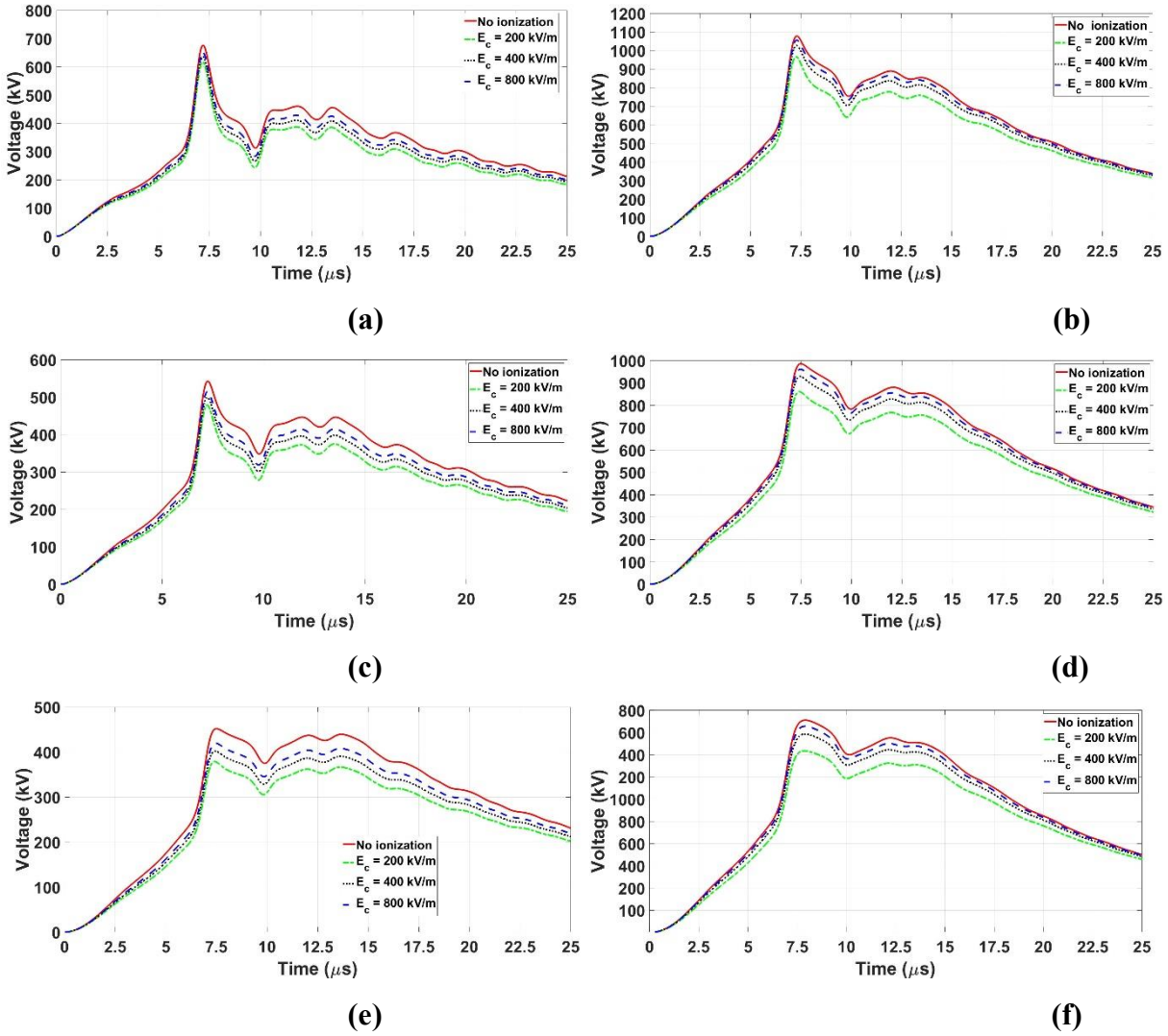

Source: Author's own work (2025).

According to this figure, it is observed that overvoltages increase with increasing soil resistivity, where the highest peak value of approximately 1.10 MV is calculated for the soil with resistivity of 4,000 Ω.m. Additionally, the overvoltages vary depending on the location of the tower arm where the point A exhibits the highest values of the overvoltages due to its proximity to the current injection point. Finally, the overvoltages waveforms obtained without

considering the ionization effect (red lines) show the highest overvoltage values, because its impulse impedance Z_p is the highest value for all cases, as confirmed by Tables 1 and 2. As the critical electric field E_c increases, the overvoltages approach those obtained when the ionization effect is neglected. Furthermore, the waveforms corresponding to the lowest critical electric field E_c = 200 kV/m exhibit the lowest overvoltage values due to the reduced impulse impedance associated with this electric field level. To quantify the differences between the overvoltages obtained with and without the ionization effect, the percentage difference (Δ_p) is calculated using the following formula:

$$\Delta_p = \frac{V_p^{\text{no ionization}} - V_p^{\text{with ionization}}}{V_p^{\text{no ionization}}} \times 100\%, \quad (16)$$

where $V_p^{\text{no ionization}}$ and $V_p^{\text{with ionization}}$ represent the overvoltage calculated for the approaches disregarding and considering the soil ionization effect (E_c = 200, 400, and 800 kV/m), respectively. The V_p corresponds to the peak value, considering the first peak of each curve for the calculation. Tables 4 and 5 show the percentage difference in the peak values of the overvoltages at points A, B and C assuming the critical electric field E_c = 200, 400 and 800 kV/m and no ionization effect for soils ρ_{soil} of 1,000 and 4,000 Ω.m.

Table 4 – Percentage difference (Δ_p) , in %, for the soil of 1,000 Ω.m

Critical Electric Field	A	B	C
200 kV/m	8.74	11.77	16.14
400 kV/m	5.91	7.97	10.93
800 kV/m	3.80	5.14	7.05

Source: Author's own work (2025).

Table 5 – Percentage difference (Δ_p) , in %, for the soil of 4,000 Ω.m

Critical Electric Field	A	B	C
200 kV/m	10.28	12.71	14.44
400 kV/m	4.69	5.81	6.58
800 kV/m	2.04	2.54	2.85

Source: Author's own work, 2025.

As shown in these tables, the soil with E_c = 200 kV/m exhibits the highest percentage variation, reaching 16.14% for soil with 1,000 Ω.m and 14.44% for soil with 4,000 Ω.m, related to the position C. This can be explained by the lowest impulse impedance Z_p associated with E_c = 200 kV/m. The increased conductor radius modifies the capacitance of the tower-footing grounding system, making the reactive component of the harmonic grounding impedance more pronounced at higher frequencies. In contrast, for E_c = 800 kV/m, the differences are the smallest, not exceeding 7.05% for soil with 1,000 Ω.m and 2.85% for soil with 4,000 Ω.m, for the same position C.

The results highlight the importance of representing soil with its realistic characteristics, considering the ionization effect associated with adequate ground-return approach for high-resistivity soils, when electromagnetic transients generated for lightning strikes are involved. The soil ionization effect must be considered under conditions conducive to electric fields surpassing the critical threshold for the formation of electric fields above the critical value, such as those generated in high lightning currents. This is particularly relevant in this type of studies showing that considerable differences on the voltages across the insulator strings can be obtained in when assuming realistic soils in the electromagnetic transient analysis.

CONCLUSIONS

This paper investigates the impact of soil ionization in the tower-footing grounding system on the overvoltages induced in the insulator string of a 138-kV overhead transmission line (OTHL) subjected to a lightning strike.

The results demonstrate the importance of accurately modelling soil characteristics, particularly considering the ionization effect, alongside an appropriate ground-return approach for high-resistivity soils, when investigating electromagnetic transients caused by lightning strikes. The ionization effect must be taken into account when system or event conditions promote electric fields that exceed the critical threshold the formation of electric fields exceeding the critical threshold, such as in the presence of high lightning currents. This study highlights that neglecting soil ionization can lead to significant discrepancies in the calculated impulse impedance, ultimately affecting the accuracy of transient responses in the simulations. Furthermore, the findings emphasize that assuming realistic soil conditions in simulations is crucial, as it significantly impacts the computed differences in the string of insulators. These results reinforce the need for comprehensive modelling approaches for soils and OHTL to ensure accurate evaluations of grounding system performance during transient conditions.

REFERÊNCIAS

ALEMI, M. R.; SADEGHI, S. H. H. and ASKARIAN-ABYANEH, H. A marching-on-in-time method of moments for transient modeling of a vertical electrode buried in a lossy medium. **IEEE Transactions on Electromagnetic Compatibility,** v. 64, n. 6, p. 2170-2178, 2022.

ALEMI, M. R.; SADEGHI, S. H. H. and ASKARIAN-ABYANEH, H. A marching-on-in-time method of moments for computation of transient potential rise of grounding grids exposed to lightning strikes. **IEEE Transactions on Electromagnetic Compatibility,** v. 65, n. 5, p. 1484-1491, 2023.

ALTAIR-HYPERWORKS, *Altair Feko*. **Altair Engineering**, 2023. [Online]. Available: https://altair.com/feko

BEZERRA, G. V. N.; MOREIRA, F. A.; FERREIRA, T. V. and ALÍPIO, R. Concrete encased grounding: Lightning response analysis considering the frequency dependence of soil. **IEEE Transactions on Electromagnetic Compatibility,** v. 66, n. 3, p. 879-889, 2024.

CARSON, J. R. Wave propagation in overhead wires with ground return. **The Bell System Technical Journal**, v. 5, n. 4, p. 539-554, 1926.

DE AZEVEDO, W. L. M.; DE ARAÚJO, A. R. J. and PISSOLATO FILHO, J. The effect of sandy soil porosity on lightning overvoltages of overhead 138 kV transmission line. **Electric Power Systems Research**, v. 220, p. 109272, 2023.

DE CONTI, A. and EMÍDIO, M. P. S. Extension of a modal-domain transmission line model to include frequency-dependent ground parameters. **Electric Power Systems Research**, v. 138, p. 120-130, 2016.

DE CONTI, A. and VISACRO, S. Analytical representation of single- and double-peaked lightning current waveforms. **IEEE Transactions on Electromagnetic Compatibility,** v. 49, n. 2, p. 448-451, 2007.

GAZZANA, D. S.; BRETAS, A. S.; DIAS, G. A. D.; TELLÓ, M.; THOMAS, D. W. P. and CHRISTOPOULOS, C. The transmission line modeling method to represent the soil ionization phenomenon in grounding systems. **IEEE Transactions on Magnetics**, v. 50, n. 2, p. 505-508, 2014.

GAZZANA, D. S.; TRONCHONI, A. B.; LEBORGNE, R. C.; BRETAS, A. S.; THOMAS, D. W. and CHRISTOPOULOS, C. An improved soil ionization representation to numerical simulation of impulsive grounding systems. **IEEE Transactions on Magnetics**, v. 54, n. 3, p. 1-4, 2017.

GRCEV, L. Impulsive efficiency of ground electrodes, **IEEE Transactions on Power Delivery**, v. 24, n. 1, p. 441-451, 2008.

GUSTAVSEN, B. and SEMLYEN, A. Rational approximation of frequency domain responses by vector fitting. **IEEE Transactions on Power Delivery**, v. 14, n. 3, p. 1052-

1061, 1999.

HE, J.; GAO, Y.; ZENG, R.; ZOU, J.; LIANG, x.; ZHANG, B.; LEE, J. and CHANG, S. Effective length of counterpoise wire under lightning current. **IEEE Transactions on Power Delivery**, v. 20, n. 2, p. 1585-1591, 2005.

HEIDLER, H. Analytische blitzstromfunktion zur lemp-berechnung. **18th ICLP**, Munich, Germany, 1985.

KISIELEWICZ, T. and CUENCA, M. Overview of transient simulations of grounding systems under surge conditions. **Energies**, v. 15, n. 20, p. 7694, 2022.

LEAL, O. E. S.; DE CONTI, A. and ZANON, F. O. S. User manual ULM-ATP Version 3.2, accessed October 08, 2024. [Online]. Available: https://github.com/zanonfelipe/ULMAtp

MEYBERG, R. A.; DE BARROS, M. T. C. and MAHSEREDJIAN, J. New methodology for representing soil ionization in fdtd simulations of grounding electrodes. **IEEE Transactions on Electromagnetic Compatibility**, 2024.

MOKHTARI, M. and GHAREHPETIAN, G. B. Integration of energy balance of soil ionization in cigre grounding electrode resistance model. **IEEE Transactions on Electromagnetic Compatibility**, v. 60, n. 2, p. 402-413, 2017.

MOKHTARI, M.; ABDUL-MALEK, Z. and GHAREHPETIAN, G. B. A critical review on soil ionization modelling for grounding electrodes. **Archives of Electrical Engineering**, p. 449-461, 2016.

MORCHED, A. GUSTAVSEN, B. and TARTIBI, M. A universal model for accurate calculation of electromagnetic transients on overhead lines and underground cables. . **IEEE Transactions on Power Delivery**, v. 14, n. 3, p. 1032-1038, 1999.

NAKAGAWA, M. Admittance correction effects of a single overhead line. **IEEE Transactions on Power Apparatus and Systems**, n. 3, p. 1154-1161, 1981.

NEKHOUL, B.; HARRAT, B.; BOUTADJINE, A. And MELIT, M. A simplified numerical modeling of the transient behavior of grounding systems considering soil ionization. **Electric Power Systems Research**, v. 211, p. 108182, 2022.

SCHROEDER, M. A. O.; MOURA, R. A.; ASSIS, F. A. and PAULINO, J. O. Evaluation of the transmission tower and frequency-dependent soil parameters influence on the grounding potential rise waveforms. **Electric Power Systems Research**, v. 222, p. 109495, 2023.

SENGAR, K. P. and CHANDRASEKARAN, K. Transient analysis of earthing electrodes considering soil ionization phenomenon under lightning impulsive condition. **Electrical Engineering**, v. 106, n. 3, p. 3083-3096, 2024.

SILVA, B. P.; VISACRO, S. and SILVEIRA, F. H. HEM-TD: New Time-Domain Eletromagnetic Model for Calculating the Lightning Response of Electric Systems and Their Components. **IEEE Transactions on Power Delivery**, v. 37, n. 6, p. 4848-4857, 2022.

SILVA, B. P.; VISACRO, S. and SILVEIRA, F. H. HEM-TD: New approaches to represent the frequency dependence of soil parameters on the time-domain hybrid electromagnetic model (HEM-TD). **IEEE Transactions Electromagnetic Compatibility**, v. 65, n. 6, p. 1793-1800, 2023.

SOUZA, R. E. The effect of soil ionization on the lightning performance of transmission lines. **2014 IEEE Internacional Conference on Lightning Protection (ICLP)**, p. 1307-1311, 2014.

XGSLab. Electromagnetic simulation for power, grounding and lightning protection systems. [Online]. Available: https://www.xgslab.com/xgslab-new/general

ZANON, F. O.; LEAL, O. E. and DE CONTI, A. Implementation of the universal line model in the alternative transients program. **Electric Power Systems Research**, v. 197, p. 107311, 2021.